

# Experimental characterization of the Gaussian state of squeezed light obtained via single-passage through an atomic vapor

P. Valente, A. Auyuanet, S. Barreiro, H. Failache, and A. Lezama\*  
*Instituto de Física, Facultad de Ingeniería, Universidad de la República,*  
*J. Herrera y Reissig 565, 11300 Montevideo, Uruguay*

(Dated: March 2, 2024)

We show that the description of light in terms of Stokes operators in combination with the assumption of Gaussian statistics results in a dramatic simplification of the experimental study of fluctuations in the light transmitted through an atomic vapor: no local oscillator is required, the detected quadrature is easily selected by a wave-plate angle and the complete noise ellipsis reconstruction is obtained via matrix diagonalization. We provide empirical support for the assumption of Gaussian statistics in quasi-resonant light transmitted through an  $^{87}\text{Rb}$  vapor cell and we illustrate the suggested approach by studying the evolution of the fluctuation ellipsis as a function of laser detuning. Applying the method to two light beams obtained by parting squeezed light in a beamsplitter, we have measured entanglement and quantum Gaussian discord.

PACS numbers: 42.50.Lc, 42.50.Dv, 42.50.Nn

## I. INTRODUCTION

It is well established that the propagation of linearly polarized continuous-wave laser light through a near resonant atomic vapor can result in squeezing of the field with polarization component orthogonal to the incident field polarization (vacuum squeezing) [1–6]. Such phenomenon has been understood as the consequence of the nonlinear response of the atomic medium giving rise to the effect of polarization self-rotation (PSR) of elliptically polarized light. PSR is the consequence of the third order susceptibility of the atomic sample. Using this susceptibility, it can be shown that the input-output relations for the quantum field operators [2] result in vacuum squeezing of the field polarized in the direction orthogonal to the incident field polarization (hereafter referred as “vacuum polarization”).

Initial work on this subject has centred the attention only on the squeezed polarization component of the field. From the experimental point of view, this required an auxiliary local oscillator to perform the balanced homodyne detection of the squeezed light. Usually, the strong linear polarization component of the field has been used as a local oscillator [2, 3, 5].

In a previous article [6], we have adopted a different point of view in which the two polarization components of the light beam are simultaneously considered. From this perspective, the squeezing effect is seen as a modification in the fluctuations of the polarization of the light i.e. the Stokes operators associated to the field. A reduction of the variance of a Stokes operator below the corresponding standard quantum limit (SQL) indicates polarization squeezing [7]. Experimentally, the main advantage of using polarization modes for the investigation of the quantum properties of light is the elimination of

the requirement of a local oscillator.

Polarization squeezing and entanglement were first obtained using two independent optical parametric amplifiers [8, 9] and a cold atomic cesium cloud inside an optical cavity [10, 11]. Taking advantage of the fact that polarization squeezing does not require a shared local oscillator, it was recently used for entanglement distribution [12] and long distance quantum communication [13].

In this article we go a step forward in the examination of the fluctuation properties of the polarization state of laser light transmitted through an atomic sample by incorporating the additional assumption of the Gaussian statistics of the quantum state of the light field. These states have a very elegant mathematical description and are simple to manipulate. Also, Gaussian states of light are commonly encountered: the vacuum and the coherent states are Gaussian and so are the squeezed vacuum and the displaced squeezed vacuum. In addition, a wide range of field evolutions are known to preserve the Gaussian nature of the field state [14]. In particular, the PSR effect results in squeezed vacuum of the vacuum polarization component. Based on the above, we have made the working assumption of the Gaussian nature of the light state. We provide experimental evidence in support of this assumption.

The purpose of this article is to show that by combining the description of the field in terms of Stokes operators and the hypothesis of Gaussian statistics one can easily have access to full information about the light state. We illustrate this possibility by studying laser frequency dependence of the squeezed and anti-squeezed quadrature variances and the corresponding quadrature angles. In the last part of the paper, we apply Gaussian analysis of Stokes operators measurements to the determination of entanglement quantifiers and quantum Gaussian discord on two light beams separated in a beamsplitter.

---

\*Electronic address: alezama@fing.edu.uy

## II. BACKGROUND

### A. Stokes operators

A quasi-monochromatic light beam propagating in the  $z$  direction is associated to the annihilation operators  $a_x$  and  $a_y$  corresponding to the  $x$  and  $y$  linear polarization components respectively. Alternatively, one can refer to a different polarization basis and introduce  $a_{1(2)} = (a_x + (-)a_y)/\sqrt{2}$  corresponding to the polarization components along the main diagonals of the  $x, y$  plane or  $a_{\pm} = (a_x \pm ia_y)/\sqrt{2}$  corresponding to the two circular polarizations components.

In order to describe the polarization state of the field it is convenient to introduce the Stokes operators:

$$S_0 = a_x^\dagger a_x + a_y^\dagger a_y = n_x + n_y \quad (1a)$$

$$S_1 = a_x^\dagger a_x - a_y^\dagger a_y = n_x - n_y \quad (1b)$$

$$S_2 = a_x^\dagger a_y + a_y^\dagger a_x = n_1 - n_2 \quad (1c)$$

$$S_3 = i(a_y^\dagger a_x - a_x^\dagger a_y) = n_- - n_+ \quad (1d)$$

where  $n_\nu \equiv a_\nu^\dagger a_\nu$  is the photon number operator associated to a given polarization. The Stokes operators  $S_{1-3}$  obey the angular-momentum-like commutation rule:

$$[S_i, S_j] = 2i\epsilon_{ijk}S_k, \quad (2)$$

where  $\epsilon_{ijk}$  is  $\pm 1$  depending on the parity of the  $i, j, k$  permutation.

It is convenient to introduce a generalized Stokes operator in the 2 – 3 plane parametrized by the angle  $\theta$ :

$$S_\theta = n_{\theta+} - n_{\theta-} = S_2 \cos(\theta) + S_3 \sin(\theta) \quad (3)$$

where  $n_{\theta\pm}$  are the photon number operators corresponding to the field operators:  $a_{\theta\pm} = (a_x \pm e^{i\theta} a_y)/\sqrt{2}$  which correspond to two orthogonal elliptical polarization components. It can be easily shown that  $S_{\theta=0} = S_2$  and  $S_{\theta=\pi/2} = S_3$ . The generalized Stokes operators verify the commutation rule:

$$[S_\theta, S_{\theta'}] = 2iS_1 \sin(\theta' - \theta) \quad (4)$$

In this article we are concerned with a field that is intense and essentially polarized along the  $x$  direction. Let  $\alpha = \langle a_x \rangle$  be the expectation value of the field operator for the  $x$  polarization. We assume that  $|\alpha| \gg |\langle a_y \rangle| \simeq 0$  and that the fluctuations of the  $x$  polarization components of the field are small compared to  $\alpha$ . Under such conditions the Stokes operators can be approximated as:

$$S_0 \simeq S_1 \simeq |\alpha|^2 \quad (5a)$$

$$S_2 \simeq \alpha^* a_y + \alpha a_y^\dagger \quad (5b)$$

$$S_3 \simeq i(\alpha a_y^\dagger - \alpha^* a_y) \quad (5c)$$

$$S_\theta \simeq \alpha^* a_y e^{-i\theta} + \alpha a_y^\dagger e^{i\theta} \quad (5d)$$

with

$$[S_\theta, S_{\theta'}] \simeq 2i|\alpha|^2 \sin(\theta' - \theta) \quad (6)$$

In particular,

$$[S_\theta, S_{\theta+\pi/2}] \simeq 2i|\alpha|^2 \quad (7)$$

which leads to the uncertainty relation:

$$\Delta S_\theta \Delta S_{(\theta+\pi/2)} \geq |\alpha|^2 \quad (8)$$

Introducing  $X_\theta \equiv S_\theta/|\alpha|$  and  $P_\theta \equiv S_{\theta+\pi/2}/|\alpha|$  we have:

$$[X_\theta, P_\theta] = 2i \quad (9)$$

which is the usual commutation rule for orthogonal quadratures. In consequence these operators must obey the Heisenberg uncertainty relation:

$$\Delta X_\theta \Delta P_\theta \geq 1 \quad (10)$$

The observables  $S_\theta$  and  $S_{\theta+\pi/2}$  as well as  $|\alpha|^2$  and therefore  $X_\theta$  and  $P_\theta$ , are accessible to measurement. In this paper we consider a phase-space description of the field state in the  $X, P$  (or  $S_\theta, S_{\theta+\pi/2}$ ) plane.

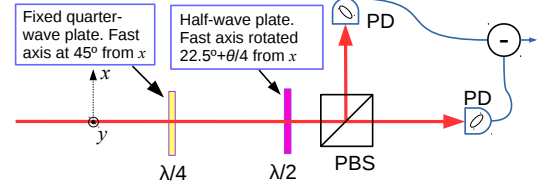


FIG. 1: (Color on-line) Experimental scheme for the measurement of the Stokes operator  $S_\theta$ . The angle  $\theta$  is selected by the orientation of the half-wave plate axis. PBS: polarization beam-splitter. PD: photodetector.

The measurement of the generalized operator  $S_\theta$  can be achieved using the arrangement shown in Fig. 1. A fixed quarter-wave plate positioned with its principal axis oriented at  $\pi/4$  with respect to the axis  $x$  is followed by a half-wave plate whose fast axis forms an angle of  $\pi/8 + \theta/4$  with respect to  $x$ . With this arrangement, the two photodetectors outputs are respectively proportional to  $n_{\theta+}$  and  $n_{\theta-}$  i.e. the photon numbers corresponding to two orthogonal elliptical polarizations. In the case of our experiment, the axis of the two ellipses are oriented at  $\pm\pi/4$  with respect to the incident polarization. In consequence, the mean value of the two photodetectors outputs are balanced. This arrangement is simpler than the one that we have previously used [6] which required a tilted waveplate and the calibration of the phase difference between orthogonal linear polarization as a function of the tilt angle.

## B. Gaussian states

In recent years, quantum information processing with continuous variables has received large attention [14]. A fundamental role is played by quantum systems prepared in Gaussian states [15, 16]. Such states have been used to demonstrate quantum correlations between two separate systems. Over the past decade, a significant amount of work has been devoted to the demonstration and measurement of entanglement using continuous variables [17–27]. More recently [28–31], Gaussian states were used in the determination of the quantum discord between two systems.

A quantum state describing a continuous variable is said to be Gaussian if its Wigner function defined over the  $X, P$  plane is Gaussian. A two-dimensional Gaussian function is entirely defined by the covariance matrix:

$$\begin{pmatrix} \Delta X^2 & \Delta XP \\ \Delta XP & \Delta P^2 \end{pmatrix} \quad (11)$$

where for any two operators  $Y, Z$  we use  $\Delta YZ \equiv \frac{1}{2} \langle YZ + ZY \rangle - \langle Y \rangle \langle Z \rangle$ .

For a given  $\theta$ , it is easily shown that the covariance matrix is given by:

$$\begin{pmatrix} \Delta X_\theta^2 & \frac{1}{2} [\Delta X_{\theta+\frac{\pi}{4}}^2 - \Delta X_{\theta-\frac{\pi}{4}}^2] \\ \frac{1}{2} [\Delta X_{\theta+\frac{\pi}{4}}^2 - \Delta X_{\theta-\frac{\pi}{4}}^2] & \Delta X_{\theta+\frac{\pi}{2}}^2 \end{pmatrix} \quad (12)$$

All terms in (12) can be experimentally measured. Once the covariance matrix is known for a given choice of the angle  $\theta$  it can be easily calculated for different angles through a rotation transform (see Eq. 3). As the value of  $\theta$  is varied, the variance  $\Delta X_\theta^2$  describes an ellipsis. For the proper choice of  $\theta$  corresponding to the orientation of one of the ellipsis main axis, the covariance matrix becomes diagonal. If  $\Delta X_\theta^2 < 1$  (see Eq. 10) the field is squeezed and the angle  $\theta$  identifies the corresponding quadrature.

For two modes ( $a$  and  $b$ ) a Gaussian state is entirely characterized by the covariance matrix:

$$\begin{pmatrix} \Delta X_a^2 & \Delta X_a P_a & \Delta X_a X_b & \Delta X_a P_b \\ \Delta P_a X_a & \Delta P_a^2 & \Delta P_a X_b & \Delta P_a P_b \\ \Delta X_b X_a & \Delta X_b P_a & \Delta X_b^2 & \Delta X_b P_b \\ \Delta P_b X_a & \Delta P_b P_a & \Delta P_b X_b & \Delta P_b^2 \end{pmatrix} \quad (13)$$

All the coefficients in (13) can be experimentally measured using the setup shown in Fig. 2. The coefficients referring to a single mode are determined as in (12). The two-mode coefficients of the covariance matrix are of the form:

$$\Delta Y_a Z_b \equiv \frac{\Delta S_{\theta a} S_{\theta' b}}{|\alpha_a \alpha_b|} \quad (14)$$

where  $|\alpha_a|^2$  and  $|\alpha_b|^2$  are given by the shot noise levels on modes  $a$  and  $b$  respectively.

Using the setup shown in Fig. 2, the variances  $\Delta(S_{\theta a} \pm S_{\theta' b})^2$ , corresponding to the sum and difference of the two balanced detectors outputs, can be measured. With the help of the identity,  $\Delta S_{\theta a} S_{\theta' b} = [\Delta(S_{\theta a} + S_{\theta' b})^2 - \Delta(S_{\theta a} - S_{\theta' b})^2]/4$  and the previously determined values of  $|\alpha_a|$  and  $|\alpha_b|$  the two-mode coefficients are readily computed.

Williamson's theorem [32] ensures that the covariance matrix can be diagonalized through the application of a symplectic transformation. Also, the covariance matrix is characterized by four invariants under symplectic transformations. The two eigenvalues of the diagonal form are the (degenerate) symplectic eigenvalues  $\nu_+$  and  $\nu_-$  which can be expressed in terms of the symplectic invariants [33]. The following properties derive from the symplectic invariants and eigenvalues.

### 1. Consistency

A covariance matrix must satisfy some constraints to represent a physical Gaussian state. In order to verify the Heisenberg uncertainty relation, the symplectic eigenvalues  $\nu_k$  must verify [34]:

$$\nu_k \geq 1 \quad (15)$$

### 2. Entanglement

The positivity of the partial transposed matrix is a necessary condition for separability [35]. It is also a sufficient condition in the case of two-mode Gaussian states [36]. If  $\tilde{\nu}_-$  and  $\tilde{\nu}_+$  with ( $\tilde{\nu}_+ > \tilde{\nu}_-$ ) are the symplectic eigenvalues of the partially transposed covariance matrix, the state is entangled if  $\tilde{\nu}_- < 1$ . In addition, the amount of entanglement can be quantified through the logarithmic negativity  $LN = -\sum_k \log(\tilde{\nu}_k)$  (the sum extending over all  $\tilde{\nu}_k < 1$ ) or  $LN = 0$  if  $\tilde{\nu}_k \geq 1, \forall k$  [37].

### 3. Quantum Gaussian discord

Entanglement does not account for all quantum correlations. In fact, quantum correlations can exist for separable mixed states. The quantum discord [38] intends to quantify quantum correlations beyond entanglement. Initially defined for discrete quantum systems, its definition was extended to Gaussian states [39, 40]. The optimality of the quantum Gaussian discord (*QGD*) is discussed in [41]. The *QGD* can be directly computed from the four symplectic invariants of the covariance matrix [40].

### III. EXPERIMENT

A scheme of the experimental setup is presented in Fig. 2. The details of the laser source and the atomic cell environment have been previously described in [6]. We remind the essential features. A 795 nm laser beam with approximately 40 mW of total power is linearly polarized and focussed with a 50 mm focal length at the center of a 5 cm long uncoated glass vapor cell containing isotopically pure  $^{87}\text{Rb}$  surrounded by a magnetic shield. The cell is heated to  $50^\circ\text{C}$ . The laser beam is re-collimated after the cell. The laser frequency can be scanned around the Rb D1 transitions.

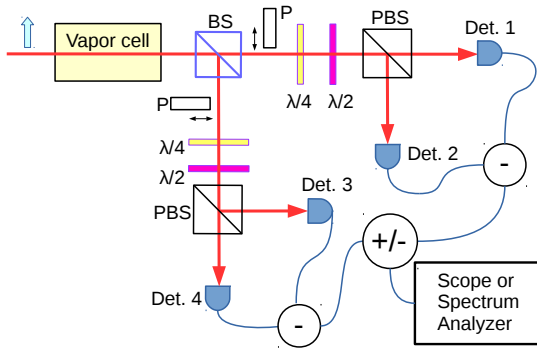


FIG. 2: (Color on-line) Experimental setup used for the characterization of a two-mode state corresponding to the output of the  $\sim 50\%$  non-polarizing beam-splitter (BS). On each output a Stokes operator measurement setup is implemented. The balanced detector outputs can be either added or subtracted for global operator measurements.

In the first set of experiments described below the beam splitter (BS) shown in Fig. 2 was not present thus directly realizing the detection arrangement presented in Fig. 1. To determine the shot-noise level, a linear polarizer is introduced on the beam path before the wave-plates. As a consequence, the light polarization perpendicular to that of the incident field is blocked and replaced by vacuum. In this case, the balanced detector output variance corresponds to  $\Delta S_\theta^2 = |\alpha|^2$  which represents the shot-noise level for the fluctuations of the Stokes operators  $S_\theta$ . In subsequent measurements, with the polarizer removed, the shot-noise level is scaled in proportion to the light intensity to account for the small attenuation introduced by the polarizer.

In a second set of experiments the *non-polarizing* beamsplitter BS was introduced. An approximately 50% transmission and reflection BS was used. Two separate balance detections were implemented to measure Stokes operators on both output ports of the beamsplitter. As a consequence of the BS being non-polarizing, the intense polarization component of the field is the same on the two outputs. The wave-plate angles are referred to this common direction. The AC outputs of the two bal-

anced detectors are either added or subtracted to access the fluctuations of global observables of the system. The total signal is sent to an oscilloscope for a time domain study of the fluctuations or to a spectrum analyser (SA) that records the noise power within a given bandwidth around a selected central frequency. The shot-noise levels corresponding the each of the light beams are independently recorded.

For a given combination of the waveplates, the laser is scanned around the D1 transitions of  $^{87}\text{Rb}$  and the corresponding fluctuations data is recorded. Using the data for the four choices of  $\theta = -\pi/4, 0, \pi/4, \pi/2$  the covariance matrix (Eq. 11) is determined as a function of the laser detuning. For each detuning the covariance matrix can be brought into its diagonal form and the minimum and maximum noise variances computed as well as the corresponding quadrature angles.

### IV. RESULTS

#### A. Gaussianity test

We have initially tested our assumption of Gaussian statistics of the light fluctuations. To assert the Gaussian nature of the field state is not a simple task [42]. We have approached this question empirically by examining the data corresponding to the balanced detector output as a function of time for different choices of the Stokes operator and the field. For each  $S_\theta$ , we have recorded 40 oscilloscope traces consisting of 2500 data points taken over a  $250\ \mu\text{s}$  time interval. Since the temporal record of the fluctuations is plagued by technical noise excess, specially at low frequency, we have numerically band-pass filtered the data string to extract the fluctuations corresponding to a specific frequency interval  $[\Omega - \Delta/2, \Omega + \Delta/2]$  where  $\Omega$  is the noise central frequency and  $\Delta$  the bandwidth. The filtering procedure consisted in Fourier transforming the data string, replacing by zeros the points corresponding to frequencies whose *absolute value* lies outside the frequency interval and performing the inverse Fourier transform.

The histogram of the filtered time domain fluctuations are presented in Fig. 3 for different choices of the Stokes operator  $S_\theta$ . The histogram of the corresponding shot noise fluctuations is also shown. All histograms are well fitted by a normalized Gaussian function with the corresponding variance. The data in Fig. 3 corresponds to a maximum squeezing of 1.6 dB with no correction for losses.

An additional test of the Gaussian statistics of the Stokes operators fluctuations results from the computation of the stochastic moments. For a Gaussian distribution, the odd moments are all zero and for  $p$  even they obey:  $\langle x^p \rangle = \langle x^2 \rangle^{\frac{p}{2}} (p-1)!!$ . Figure 4 shows the comparison of the statistical moments of the recorded data to the corresponding value for a Gaussian distribution for moments up to  $p = 6$ . The odd moments are zero

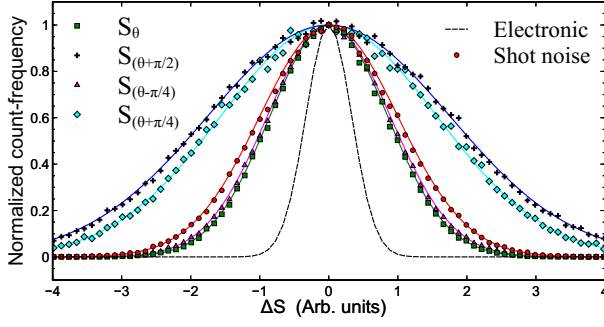


FIG. 3: (Color on-line) Symbols: Normalized histograms of the measurement of the filtered ( $\Omega = 3$  MHz,  $\Delta = 400$  kHz) fluctuations of the Stokes operators. Solid lines: Gaussian functions with the same variance than the corresponding data. Dashed line: Residual electronic-noise level. The laser is tuned near the  $^{87}\text{Rb}$   $F_g = 2 \rightarrow F_e = 2$  transition at the position of maximum squeezing.

within the measurement uncertainty and the even moments differ from the expecting Gaussian value in less than 8%.

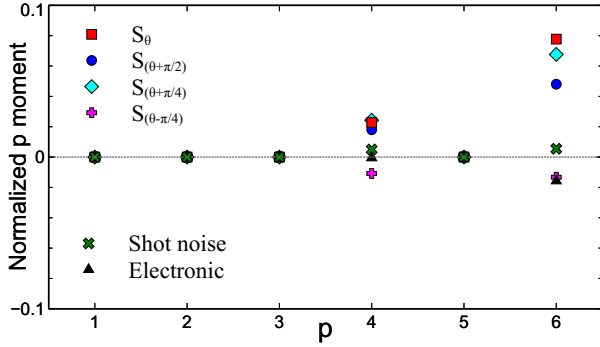


FIG. 4: (Color on-line) Normalized statistical moments for the measurements of Stokes operators. The normalized moment of order  $p$  is defined as:  $\langle x^p \rangle / [\langle x^2 \rangle^{p/2} (p-1)!!] - \varepsilon_p$  where  $\varepsilon_p = 1$  if  $p$  is even and zero otherwise. Here  $x$  represents the result of a measurement. The normalized moments are zero for a Gaussian distribution.

Supported on these observations, we conclude that the assumption of Gaussian nature of the field state is reasonable in the context of this work.

### B. Single Stokes operator

Figure 5 presents the noise power (recorded with a spectrum analyser) around 2.7 MHz (resolution bandwidth 100 KHz) of a single Stokes operator as a function of laser detuning. In Fig. 5,  $S_\theta$  was chosen to correspond to the maximum squeezing occurring near the  $F = 2 \rightarrow F' = 2$  transition. Smaller squeezing is also observed around the  $F = 1 \rightarrow F'$  transitions. For other

laser detunings the fluctuations of  $S_\theta$  are above the shot-noise level. It is worth noticing the broad frequency range for which the light fluctuations are affected by the atomic transitions. It extends over a range of around 17 GHz, much larger than the total D1 absorption spectrum of rubidium. A slow decrease of the excess noise structure with the laser detuning from atomic resonances was predicted by the numerical simulations reported in [4].

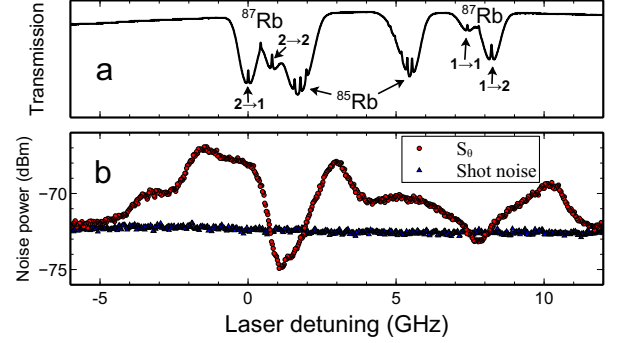


FIG. 5: (Color on-line) a) Reference-cell saturated-absorption signal used for frequency calibration. The hyperfine transitions of the  $^{87}\text{Rb}$  D1 line are indicated. b) Circles: Noise power at 2.7 MHz for the Stokes operator  $S_\theta$  presenting maximum squeezing around the  $F = 2 \rightarrow F' = 2$  transition in a cell containing isotopically pure  $^{87}\text{Rb}$ . Triangles: Shot noise level.

### C. Phase-space description of one field

In order to have access to the covariance matrix, we have recorded with a spectrum analyser (central frequency 2.7 MHz, resolution bandwidth 100 kHz) the fluctuations of the four Stokes operators  $S_{\theta-\pi/4}, S_\theta, S_{\theta+\pi/4}, S_{\theta+\pi/2}$ . For convenience we chose  $S_\theta$  to correspond to  $S_3$ . The covariance matrix was constructed according to (12) and diagonalized to identify the minimum and maximum noise variances and the corresponding quadrature angle. The results are presented in Fig. 6 (see also [43]). Similar spectra of the minimum and maximum noise variances were presented in [3–5]. Notice the considerable simplification arising from the combination of Stokes operators detection and Gaussian analysis. In [3, 4], a sophisticated active stabilization of the phase of the local oscillator was implemented in order to track the field quadrature corresponding to maximum or minimum noise. In [5] this was achieved manually for a discrete number of laser detunings. Also these articles did not report the determination of the quadrature angle corresponding to squeezing possibly due to difficulties in the local oscillator phase calibration in the interferometric setup. By contrast, in our setup there are no interferometric instabilities affecting the choice of  $S_\theta$ , no stabilization loop is required since the data is recorded for a fixed value of the angle  $\theta$  and the determination

of the noise variances and corresponding quadrature angles readily arise from the numerical covariance matrix diagonalization.

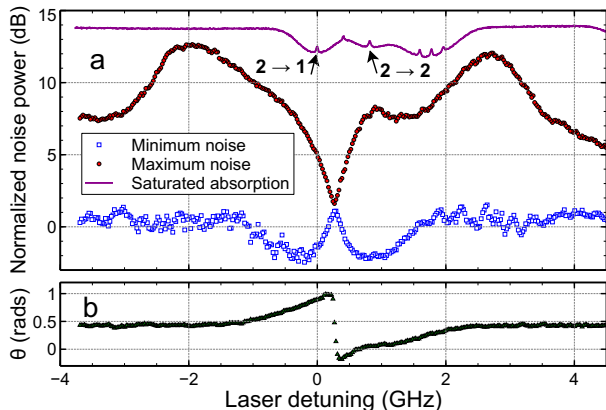


FIG. 6: (Color on-line) (a) Quadrature noise power normalized to the shot-noise level as a function of laser detuning. Squares: Minimum quadrature noise. Circles: Maximum quadrature noise. Solid: Reference saturated absorption signal with relevant  $^{87}\text{Rb}$  D1 transitions indicated. (b) Quadrature angle corresponding to the minimum noise. (See also [43]).

The results presented in Fig. 6 reveal interesting features about the noise structure. As previously observed [3–6], squeezing is present around the  $F = 2 \rightarrow F' = 1$  and  $F = 2 \rightarrow F' = 2$  albeit for different quadrature angles. Interestingly enough, for the laser detunings where squeezing does not occur, the minimum noise variance remains close to the shot-noise level. On the other hand the maximum noise variance presents excess noise above the limit imposed by the Heisenberg uncertainty relation.

Perhaps the more interesting feature in Fig. 6 is the existence of a laser frequency between the two hyperfine transitions for which the maximum and minimum noise variances are nearly equal and very close to the shot-noise level. The existence of this singular point in the noise spectrum can be related to the cancellation of the PSR effect around this position [1]. It is interesting to notice that not only the squeezing is suppressed but very little excess noise is added by the atomic interaction. The squeezing occurs on either side of such noise cancellation point.

Our method readily allows the observation of the rotation of the Stokes operator quadrature noise ellipsis as a function of laser detuning [43]. A steep variation of the orientation of the noise ellipsis over 72 degrees occurs around the noise cancellation point. It was recently suggested [44, 45] that the control of the orientation of squeezed light noise ellipsis could be applied to precision improvement in gravitational wave detection interferometry. Rotation of the noise ellipsis was recently observed in squeezed light generated via four-wave-mixing in an atomic system [46].

#### D. Two-field state characterization

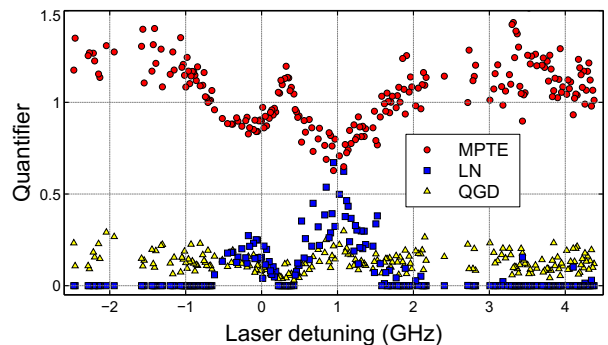


FIG. 7: (Color on-line) Two-mode state quantifiers for the two beamsplitter outputs as a function of laser detuning. Circles: minimum partial transpose eigenvalue ( $MPTE \equiv \tilde{\nu}_-$ ). Squares: logarithmic negativity ( $LN$ ). Triangles: quantum Gaussian discord ( $QGD$ ).

We have recorded the covariance matrix of the compound system for each value of the laser detuning following the procedure described in Section II B.

Since the experimentally determined covariance matrix is affected by noise, we have tested each covariance matrix for consistency and physical significance. We have discarded all the covariance matrices that did not satisfy the physical consistency requirement (Eq. 15). The data complying to this requirement was used for symplectic invariants determination and computation of the symplectic eigenvalue  $\equiv \tilde{\nu}_-$ , the logarithmic negativity and the quantum Gaussian discord between modes  $a$  and  $b$  conditioned to measurements on  $b$  [40].

The results are presented in Fig. 7. In spite of the significant amount of noise, the positivity of the partial transpose criterion and the logarithmic negativity indicate entanglement near the laser frequency range for which squeezing is present on single field Stokes operators (see Fig. 6). Notice that nonzero quantum Gaussian discord occur in all the laser frequency range shown in Fig. 7 indicating that the two-mode state presents some amount of nonclassical correlations even when it is separable.

As a final remark, it is worth mentioning that the experimental procedure described above is independent of the intensity balance of the two outputs of the BS. Such balance will nevertheless have an influence on the entanglement and quantum Gaussian discord observed.

#### V. CONCLUSIONS

We have shown that the description of the field in terms of polarization (Stokes) states in combination with the assumption of Gaussian statistics results in considerable simplification of the study of the quantum state of

light transmitted through an atomic sample: The experimental setup is dramatically reduced. All interferometric instabilities are removed. The selection of the detected phase space quadrature corresponds to the rotation angle of a single waveplate. Finally, the complete state (noise ellipsis) reconstruction is computed through matrix diagonalization.

Taking advantage of this simplicity, we have presented, for the first time to our knowledge, the complete evolution of the noise ellipsis describing light fluctuations around a given central frequency as a function of laser detuning. In the case of two light modes, obtained by parting a squeezed light beam in a beamsplitter, the use

of Gaussian states formalism in combination with Stokes operator observations, allowed us to demonstrate entanglement and measure the quantum Gaussian discord indicating that the generated light states could be suitable for quantum information processing.

## VI. ACKNOWLEDGMENTS

We wish to thank P. Nussenzveig for useful suggestions. This work was supported by CSIC and ANII.

- 
- [1] A. B. Matsko, I. Novikova, G. R. Welch, D. Budker, D. F. Kimball, and S. M. Rochester, *Physical Review A (Atomic, Molecular, and Optical Physics)* **66**, 043815 (pages 10) (2002), URL <http://link.aps.org/abstract/PRA/v66/e043815>.
  - [2] J. Ries, B. Brezger, and A. I. Lvovsky, *Phys. Rev. A* **68**, 025801 (2003).
  - [3] E. E. Mikhailov and I. Novikova, *Opt. Lett.* **33**, 1213 (2008), URL <http://ol.osa.org/abstract.cfm?URI=ol-33-11-1213>.
  - [4] E. E. Mikhailov, A. Lezama, T. W. Noel, and I. Novikova, *JMO* **56**, 1985 (2009).
  - [5] I. H. Agha, G. Messin, and P. Grangier, *Opt. Express* **18**, 4198 (2010).
  - [6] S. Barreiro, P. Valente, H. Failache, and A. Lezama, *Phys. Rev. A* **84**, 033851 (2011), URL <http://link.aps.org/doi/10.1103/PhysRevA.84.033851>.
  - [7] N. Korolkova, G. Leuchs, R. Loudon, T. C. Ralph, and C. Silberhorn, *Phys. Rev. A* **65**, 052306 (2002).
  - [8] W. P. Bowen, N. Treps, R. Schnabel, and P. K. Lam, *Phys. Rev. L* **89**, 253601 (2002).
  - [9] W. P. Bowen, R. Schnabel, Hans-A. Bachor, and P. K. Lam, *Phys. Rev. Lett.* **88**, 093601 (2002).
  - [10] V. Josse, A. Dantan, L. Vernac, A. Bramati, M. Pinard, and E. Giacobino, *Phys. Rev. Lett.* **91**, 103601 (2003).
  - [11] V. Josse, A. Dantan, A. Bramati, and E. Giacobino, *J. Opt. B: Quantum Semiclass. Opt.* **6**, S532S543 (2004).
  - [12] C. Peuntinger, V. Chille, L. Mišta, N. Korolkova, M. Förtsch, J. Korger, C. Marquardt, and G. Leuchs, *Phys. Rev. Lett.* **111**, 230506 (2013), URL <http://link.aps.org/doi/10.1103/PhysRevLett.111.230506>.
  - [13] C. Peuntinger, B. Heim, C.R. Müller, C. Gabriel, C. Marquardt, and G. Leuchs, *Phys. Rev. Lett.* **113**, 060502 (2014), URL <http://link.aps.org/doi/10.1103/PhysRevLett.111.230506>.
  - [14] S. L. Braunstein and P. van Loock, *Rev. Mod. Phys.* **77**, 513 (2005).
  - [15] C. Weedbrook, S. Pirandola, R. Garcia-Patron, N. J. Cerf, T. C. Ralph, J. H. Shapiro, and S. Lloyd, *Rev. of Mod. Phys.* **84**, 624 (2012).
  - [16] A. Ferraro, S. Olivares, and M. G. Paris, *Gaussian states in quantum information* (Bibliopolis, Napoli, 2005), ISBN 88-7088-483-X, OSSE URL <http://www.bibliopolis.it>.
  - [17] L. M. Duan, G. Giedke, J. I. Cirac, and P. Zoller, *Phys. Rev. Lett.* **84**, 2722 (2000).
  - [18] J. Laurat, G. Keller, J. A. Oliveira-Huguenin, C. Fabre, T. Coudreau, A. Serafini, G. Adesso, and F. Illuminati, *J. Opt. B: Quantum Semiclass. Opt.* **7**, S577 (2005).
  - [19] V. D'Auria, S. Fornaro, A. Porzio, S. Solimeno, S. Olivares, and M. G. A. Paris, *Phys. Rev. Lett.* **102**, 020502 (2009), URL <http://link.aps.org/doi/10.1103/PhysRevLett.102.020502>. OSSE
  - [20] M. Yukawa, R. Ukai, P. van Loock, and A. Furusawa, *Phys. Rev. A* **78**, 012301 (2008).
  - [21] B. Hage, A. Samblowski, J. DiGuglielmo, A. Franzen, J. Fiursek, and R. Schnabel, *Nat. Phys.* **4**, 915 (2008).
  - [22] H. Yonezawa, T. Aoki, and A. Furusawa, *Nature* **431**, 430 (2004).
  - [23] H. Yonezawa, A. Furusawa, and P. van Loock, *Phys. Rev. A* **76**, 032305 (2007).
  - [24] J. DiGuglielmo, B. Hage, A. Franzen, J. Fiursek, and R. Schnabel, *Phys. Rev. A* **76**, 012323 (2007).
  - [25] X. Su, Y. Zhao, S. Hao, X. Jia, C. Xie, and K. Peng, *Opt. Lett.* **37**, 5178 (2012).
  - [26] T. Aoki, N. Takei, H. Yonezawa, K. Wakui, T. Hiraoka, A. Furusawa, and P. van Loock, *Phys. Rev. Lett.* **91**, 080404 (2003).
  - [27] R. Ukai, N. Iwata, Y. Shimokawa, S. C. Armstrong, A. Politi, J.-i. Yoshikawa, P. van Loock, and A. Furusawa, *Phys. Rev. Lett.* **106**, 240504 (2011).
  - [28] L. S. Madsen, A. Berni, M. Lassen, and U. L. Andersen, *Phys. Rev. Lett* **109**, 030402 (2012).
  - [29] R. Blandino, M. G. Genoni, J. Etesse, M. Barbieri, M. G. A. Paris, P. Grangier, and R. Tualle-Broui, *Phys. Rev. Lett.* **109**, 180402 (2012).
  - [30] U. Vogl, R. T. Glasser, Q. Glorieux, J. B. Clark, N. V. Corzo, and P. D. Lett, *Phys. Rev. A* **87**, 010101(R) (2013).
  - [31] S. Hosseini, S. Rahimi-Heshari, J. Y. Haw, S. M. Assad, H. M. Chrzanowsky, J. Janousek, T. Symul, T. C. Ralph, and P. K. Lam, *J. Phys. B: At. Mol. Opt. Phys* **47**, 025503 (2014).
  - [32] J. Williamson, *Am. J. Math.* **58**, 141 (1936).
  - [33] A. Serafini, F. Illuminati, M. G. A. Paris, and S. De Siena, *Phys. Rev. A* **69**, 022318 (2004).
  - [34] G. Adesso, S. Ragy, and A. R. Lee, *Open Syst. Inf. Dyn.* **21**, 1440001 (2014).
  - [35] R. Simon, *Phys. Rev. Lett.* **84**, 2726 (2000).
  - [36] R. F. Werner and M. M. Wolf, *Phys. Rev. Lett.* **86**, 3658

- (2001).
- [37] G. Vidal and R. F. Werner, Phys. Rev. A. **65**, 032314 (2002).
  - [38] H. Ollivier and W. H. Zurek, Phys. Rev. Lett. **88**, 017901 (2001).
  - [39] P. Giorda and M. G. A. Paris, Phys. Rev. Lett. **105**, 020503 (2010).
  - [40] G. Adesso and A. Datta, Phys. Rev. Lett. **105**, 030501 (2010).
  - [41] S. Pirandola, G. Spedalieri, S. L. Braunstein, N. J. Cerf, and S. Lloyd, Phys. Rev. Lett. **113**, 140405 (2014), URL <http://link.aps.org/doi/10.1103/PhysRevLett.113.140405>.
  - [42] A. Coelho, F. Barbosa, K. Cassemiro, M. Martinelli, A. Villar, and P. Nussenzveig, arXiv preprint arXiv:1502.01759 (2015).
  - [43] See Supplemental Material at <http://www.fing.edu.uy/if/optica/NoiseEllipsis.mp4> for an animation movie showing the evolution of the quadrature noise ellipsis corresponding to the data of Fig. 6. as a function of laser detuning.
  - [44] H. J. Kimble, Y. Levin, A. B. Matsko, K. S. Thorne, and S. P. Vyatchanin, Phys. Rev. D **65**, 022002 (2001), URL <http://link.aps.org/doi/10.1103/PhysRevD.65.022002>.
  - [45] T. Horrom, G. Romanov, I. Novikova, and E. E. Mikhailov, Journal of Modern Optics **60**, 43 (2013).
  - [46] N. V. Corzo, Q. Glorieux, A. M. Marino, J. B. Clark, R. T. Glasser, and P. D. Lett, Physical Review A **88**, 043836 (2013).